HHS Public Access

Author manuscript

Biol Psychiatry. Author manuscript; available in PMC 2016 June 01.

Published in final edited form as:

Biol Psychiatry. 2015 June 1; 77(11): 959–968. doi:10.1016/j.biopsych.2014.09.006.

Altered Glutamate Protein Co-Expression Network Topology Linked to Spine Loss in the Auditory Cortex of Schizophrenia

Matthew L. MacDonald[a], **Ying Ding**[b], **Jason Newman**[a], **Scott Hemby**[c,d], **Peter Penzes**[e,f], **David A. Lewis**[a], **Nathan Yates**, and **Robert A. Sweet**[a,g,h]

[a]Department of Psychiatry, University of Pittsburgh, Pittsburgh, PA

[b]Department of Biostatistics, University of Pittsburgh, Pittsburgh, PA

[c]Neuroscience Program, Wake Forest University School of Medicine, Winston-Salem, NC

[d]Department of Physiology & Pharmacology, Wake Forest University School of Medicine, Winston-Salem, NC

[e]Department of Physiology, Northwestern University Feinberg School of Medicine, Chicago, Il

[f]Department of Psychiatry and Behavioral Sciences, Northwestern University Feinberg School of Medicine, Chicago, Il

[g]VISN 4 Mental Illness Research, Education and Clinical Center (MIRECC), VA Pittsburgh Healthcare System, Pittsburgh, PA

[h]Department of Neurology, University of Pittsburgh, Pittsburgh, PA

Abstract

Background—Impaired glutamatergic signaling is believed to underlie auditory cortex pyramidal neuron dendritic spine loss and auditory symptoms in schizophrenia. Many schizophrenia risk loci converge on the synaptic glutamate signaling network. We therefore hypothesized that alterations in glutamate signaling protein expression and co-expression network features are present in schizophrenia.

Corresponding Author: Biomedical Science Tower, Rm. W-1645, 3811 O'Hara Street, Pittsburgh, PA 15213, Phone: 412-383-8548, Fax 412-624-9910, sweetra@upmc.edu.

Note The raw peptide expression data, as light/heavy ratios, is available by request to the corresponding author.

Data included here have previously been presented as abstracts in preceding of The Society for Neuroscience, The American Society of Mass Spectrometry and The American College of Neuropsychopharmacology.

The content is solely the responsibility of the authors and does not necessarily represent the official views of the National Institute of Mental Health, the National Institutes of Health, the Department of Veterans Affairs, or the United States Government.

Financial Disclosures

DAL currently receives investigator-initiated research support from the Bristol-Myers Squibb Foundation, Bristol-Myers Squibb, Curridium Ltd, and Pfizer and in 2007 to 2010 served as a consultant in the areas of target identification and validation and new compound development to AstraZeneca, BioLine RX, Bristol-Myers Squibb, Hoffman-Roche, Lilly, Merck, Neurogen, and SK Life Science. MLM, YD, JN, SH, PP NY and RAS report no biomedical financial interests or potential conflicts of interest.

Methods—Gray matter homogenates were prepared from auditory cortex grey matter of 22 schizophrenia and 23 matched controls, a subset of whom had been previously assessed for dendritic spine density. 155 selected synaptic proteins were quantified by targeted mass spectrometry. Protein co-expression networks were constructed using Weighted Gene Co-Expression Network Analysis.

Results—Proteins with evidence for altered expression in schizophrenia were significantly enriched for *Glutamate Signaling Pathway* proteins (GRIA4, GRIA3, ATP1A3 and GNAQ). Synaptic protein co-expression was significantly decreased in schizophrenia with the exception of a small group of postsynaptic density proteins, whose co-expression increased and inversely correlated with spine density in schizophrenia subjects.

Conclusions—We observed alterations in the expression of *Glutamate Signaling Pathway* proteins. Among these, the novel observation of reduced ATP1A3 expression is supported by strong genetic evidence indicating it may contribute to psychosis and cognitive impairment phenotypes. The observations of altered protein network topology further highlights the complexity of glutamate signaling network pathology in schizophrenia and provides a framework for evaluating future experiments to model the contribution of genetic risk to disease pathology.

Keywords

Schizophrenia; Postmortem; Auditory Cortex; Proteomics; Glutamate; Spine

Background

Individuals with schizophrenia (SCZ) display auditory symptoms associated with altered activation of the primary auditory cortex (AI) including auditory hallucinations(1–5). Additionally, they manifest impairments in the processing of sensory information within the AI that contribute to disease burden. For example, a reduction in the ability to discriminate tones(6–9) impacts interpretation of spoken emotion (prosody)(10, 11), impairing social cognition(12, 13). Likewise, deficits in auditory event-related potentials, such as reduced amplitude of mismatch negativity, are present in SCZ(6, 7, 14, 15). Impairments in tone discrimination and mismatch negativity are correlated and likely involve the same intracortical circuits(8) in Al layer 3(16, 17).

Several lines of evidence suggest that disrupting glutamate signaling in the AI can induce or exacerbate these auditory impairments. NMDA receptor antagonists produce reductions in mismatch negativity amplitude in normal human subjects, non-human primates(17), and mice(18–20). Similarly, NMDA receptor antagonists exacerbate psychotic symptoms in individuals with schizophrenia, including recurrence (or intensification) of auditory hallucinations(21). The role of glutamate signaling network impairments in SCZ is supported by findings that postsynaptic genes involved in NMDA and AMPA receptor signaling are significantly enriched for mutations in disease(22–25). However, these SCZ risk genes have not yet been linked specifically to auditory impairments in SCZ, despite evidence for heritability of some of these impairments(26).

Structural impairments of glutamatergic layer 3 pyramidal neurons, such as reduced dendritic spine density, are among the most consistently observed findings in postmortem

studies of individuals with SCZ(27) and have been reported in multiple brain regions, including Al(28–36). As dendritic structural features are critical for signal processing(37–40), it has been postulated that this spine loss underlies the Al processing deficits observed in SCZ. Not surprisingly then, numerous studies have demonstrated that attenuating pre- or post- synaptic glutamate signaling can decrease dendritic spine density(41–45). Surgical deafferentation of glutamatergic projections(43–45), or knockout of glutamate release proteins, results in decreased density of spines(46, 47). Postsynaptically, pharmacological blockade or knockout of glutamate receptors (AMPA or NMDA) results in decreased spine density(41–45), as does decreasing levels of the NMDA receptor co-agonist d-serine(48).

We therefore hypothesized that alterations in glutamate signaling protein expression are present in the AI of SCZ subjects. In addition, as emerging genetic data indicate that many SCZ-associated loci converge on the glutamate signaling network, we further hypothesized that alterations in network features would also be present in the AI of SCZ subjects. We tested these hypotheses using a Liquid Chromatography - Selected Reaction Monitoring/ Mass Spectrometry (LC-SRM/MS) targeted proteomics approach (49), to quantify the expression of 155 synaptic proteins in Al grey matter homogenates from 22 SCZ and 23 matched control subjects. Functional Gene Annotation analysis in DAVID(50), was used to determine if proteins with altered expression were enriched for terms related to function and cellular compartment, while Weighted Gene Co-expression Network Analysis (WGCNA) was used to investigate patterns of co-regulated protein expression. Differentially expressed proteins were enriched for the Gene Ontology term *Glutamate Signaling Pathway*. Analysis of protein co-expression network topology revealed a significant loss of correlated protein expression in SCZ. The exception to this loss was a small module of post-synaptic density proteins whose co-expression increased in SCZ. The averaged expression of these proteins was significantly inversely correlated with spine density, in the subset of SCZ subjects for which Al layer 3 spine density had previously been determined(51).

Methods

Subjects

Brain specimens from all subjects were obtained during autopsies conducted at the Allegheny County Office of the Medical Examiner after receiving consent from the next-of-kin. An independent panel of experienced clinicians made consensus Diagnostic and Statistical Manual of Mental Disorders Fourth Edition (DSM-IV) diagnoses using a previously described method(52). 22 subjects diagnosed with SCZ and 23 control subjects for which total protein extracted from AI gray matter was available were studied. Every effort was made to balance these two groups by age, sex, race, and PMI (Table 1, Supplemental Table S1). Control subjects underwent identical assessments and were determined to be free of lifetime psychiatric illness. Procedures were approved by the University of Pittsburgh Institutional Review Board and Committee for Oversight of Research Involving the Dead.

Rhesus Monkeys

The tissue utilized here has been extensively described elsewhere(53, 54). Briefly: Rhesus monkeys (3–8 years of age) were randomly assigned to one of three treatment groups: vehicle (5 male, 5 female), clozapine 5.2 mg/kg daily (5 male, 5 female), haloperidol 0.14 mg/kg daily (5 male, 5 female). Later a fourth group was treated with a higher dose of haloperidol 2.0 mg/kg twice daily (4 male, 4 female). Drugs were administered in either peanut butter or fruit treats and all animals were treated for six months.

Sample preparation and LC-SRM/MS

Human—Grey matter was harvested as previously described(55, 56): Tissue slabs containing the superior temporal gyrus with Heschl's Gyrus (HG) located medial to the planum temporal were identified, and the superior temporal gyrus removed as single block. The samples were then distributed in a block design for preparation and analysis to evenly distribute SCZ and control samples and blind the experimenters during sample preparation, analysis, and peak integration. Grey matter was collected from HG by taking 40 μm sections, and frozen at −80°C(55). Total protein was extracted using SDS extraction buffer (0.125 M Tris–HCl (pH 7), 2% SDS, and 10% glycerol) at 70 °C, and protein concentration measured by bicinchoninic acid assay in triplicate (BCA™ Protein Assay, Pierce). 20 μg of these grey matter homogenates were mixed with 10 μg of Lysine $^{13}C_6$ Stable Isotope Labeled Neuronal Proteome Standard ($^{13}C_6$STD) and processed for LC-SRM/MS analysis by on-gel trypsin digestion as previously described(49). Variability of peptide and protein quantification was assessed as described in MacDonald et al. 2013(49). Briefly, four 10 μg aliquots from the same Al grey matter homogenate were prepared and analyzed by LC-SRM/MS. For details on LC-SRM/MS, see Supplemental Methods.

Statistical Analysis

For each peptide light/heavy ratio, an Analysis of Covariance (ANCOVA) model was fitted to compare SCZ versus control. Age, postmortem interval (PMI), and assay group were adjusted in the model. In addition, there was a small, albeit statistically significant difference in pH between groups, so pH was also included in the model. The ratio (between SCZ and control) and the corresponding p-value were reported from each ANCOVA analysis. Similar analysis was performed for each protein abundance measure as well.

Pathway Analysis

Proteins were ranked by the p-value from the above ANCOVA analysis. Proteins with a p-value < .1, indicating suggestive evidence for differential levels in SCZ, were identified (Table 2). The ranked protein list was then submitted, as a list of official gene symbols, to the DAVID Functional Annotation Tool(57), and searched for Kyoto Encyclopedia of Genes and Genomes (KEGG) pathway and gene ontology (GO) term enrichment. In a first analysis the human genome was used as the background, in a second the full list of quantified proteins, submitted as non-redundant International Protein Index (IPI) identification numbers, served as the background to increase stringency.

Network Analyses

Co-expression networks were constructed by adapting the Weighted Gene Co-expression Network Analysis (WGCNA) approach(58) to study the synaptic proteome network alterations in SCZ using protein measures. Two separate networks, one for SCZ and one for control, were then visualized with nodes representing proteins and edges determined by pairwise correlations between protein abundance measures (Figure 1). The tuning parameters of these two networks were set to the same values (e.g., the power of the co-expression similarity, the minimum model size and etc.) to allow for a fair comparison of network topologies between the two cohorts. Specifically, weighted node connectivity ranged between 0 and 1 with a higher value indicating stronger connectivity between a protein and the rest of all proteins in the network. 0.15 was chosen as a cut off for inclusion in the visualized network, yielding roughly 15% of proteins assayed appearing in the SCZ network. WGCNA identified distinct modules within the networks. Module membership was characterized for Gene Ontology terms by functional enrichment using DAVID(57) and for cellular compartment enrichment using data from our previous analysis of synaptic microdomain protein enrichment in human postmortem brain tissue using Fisher's exact test(49).

Detailed descriptions of Rhesus monkey tissue preparation, LC-SRM/MS, protein/peptide selection, and data processing can be found in Supplemental Methods.

Results

Analytical Precision

The mean coefficient of variation (CV) for protein quantification was 2.6% (Supplemental Figure S1). Analytical CVs for significantly differentially expressed proteins are reported in Table 2.

Differentially expressed proteins and pathways

Out of the 289 peptides from 180 proteins assayed, 223 peptides from 155 proteins survived peptide quality control as described above. Of these 155 proteins, 17 proteins showed suggestive evidence for differential levels in SCZ (p-value < 0.1, Table 2, for p-values of individual peptides see Supplemental Table S2). Functional annotation analysis in DAVID(57) revealed that this list was significantly enriched for the GO term *Glutamate Signaling Pathway* (GRIA3, GRIA4, ATP1A3, and GNAQ, $p = 2.5E^{-6}$, Benjamini–Hochberg $q = 1.5E^{-3}$). This GO pathway is narrowly defined by glutamate receptors and their immediate signaling partners. Results remained unchanged when using a p-value < 0.05 to select proteins for DAVID analysis. A more stringent DAVID analysis of the p-value < 0.1 list, limiting the background to the 155 synaptic proteins assayed, continued to identify significant enrichment of the same proteins/pathway (p = 0.0021, Benjamini–Hochberg q = 0.02).

Co-expression network analysis

We first calculated the co-expression between all pairwise proteins for the SCZ and control cohorts separately (Supplemental Figure S2A & B) and then constructed co-expression

networks (Figure 1 A & B, Supplemental Table S3). The control network was composed of three distinct modules (Figure 1A). The Blue module was enriched for the GO term *Clathrin Coated Vesicle Membrane* (p = 0.037) and a significant number of the proteins were enriched in vesicular membrane biochemical fractions (Fisher's Exact p = 0.0041). The Turquoise module was enriched for the GO terms *NAD or NADH Binding* (p = 0.025) and *Catabolic Process* (p = 0.062) and a significant number of its proteins were enriched in cytoplasmic fractions (Fisher's Exact p = 0.0001). The Brown module was enriched for the GO Term *Regulation of Cell Death* (p = 0.029).

Visual inspection of the two networks suggests that the control network is larger and more interconnected than the SCZ network. This observation was borne out by formal testing of node connectivity: The distribution of Node Degree scores for all proteins was plotted (Supplemental Figure S3A), where Node Degree equals the number of connections each protein has to other proteins within the visualized network (Figure 1). Next, the difference in Node Degree between control and SCZ for each protein was calculated and plotted (Supplemental Figure S3B). The mean Node Degree difference between control and SCZ was −1.8. Finally, the mean Node Degree differences calculated from 1000 permutations of subject diagnosis was calculated and plotted (Supplemental Figure S3C), revealing that a mean Node Degree difference of −1.8 is significant ($p_{permuted} = 0.015$). The difference in Node Degree scores between the SCZ and control networks was also calculated for individual proteins (Supplemental Tables S4 and S5). Significance of these differences was calculated using the same permutation statistic described above. 18 proteins in the control network had significant increases in Node Degree relative to their corresponding values in the SCZ network (Supplemental Table S4).

The exception to this overall reduction in connectivity in SCZ was the Red module, present in SCZ, but not in control (Figure 1B). DAVID analysis of the 4 core Red module proteins revealed them to be enriched for the GO term *Postsynaptic Density* (p = 0.004). In the SCZ network, three proteins had significantly increased Node Degrees relative to the control network, two of which, ANK1 and ANK2, are members of the Red module unique to the SCZ network (Figure 1B, Supplemental Table S5). To further explore this emergent module, the threshold of node connectivity parameter was loosened (from 0.15 to 0.1), resulting in the visualization of additional proteins co-expressed with the 4 core proteins of this module (Figure 2A). The average expression of proteins in this module was plotted against spine density in 16 SCZ and 16 control subjects for which we have that data (Figure 2B and 2C). This comparison revealed a significant negative correlation between average protein expression and spine density (r = −.72, p = 0.0018) in SCZ (Figure 2B), but not controls (Figure 2C). Functional annotation analysis of this expanded Red module in DAVID returned enrichments for the Gene Ontology terms *Cytoskeleton* (p = 0.00076) *Synapse* (p = 0.014), and *Postsynaptic Density* (p = 0.03).

Antipsychotic Drug Treated Rhesus Monkeys

Expression of the four *Glutamate Signaling Pathway* proteins altered in SCZ (GRIA3, GRIA4, ATP1A3, and GNAQ) was investigated in cerebral cortex tissue of antipsychotic treated monkeys to determine if neuroleptics could explain these differences. GRIA4

expression levels, decreased in SCZ, were not impacted by haloperidol in rhesus monkeys and were significantly increased by clozapine (Figure 3A). GRIA3 showed a similar pattern, although the increase by clozapine did not reach significance (Figure 3B). ATP1A3 expression, also decreased in SCZ, was significantly increased by both clozapine and haloperidol (Figure 3C). GNAQ, increased in SCZ, was unchanged by clozapine and showed a trending significant decrease by haloperidol (Figure 3D).

Role of other potential confounds

In addition to antipsychotic medication, several other potential confounding factors were present in this cohort, including smoking tobacco, death by suicide, alcohol, substance abuse at time of death, and schizoaffective disorder. We did not observe a significant effect of any of these factors on the expression of the top proteins (Supplemental Table S6).

Discussion

We hypothesized that alterations to glutamate signaling protein expression and protein network features would be present in the Al of SCZ patients. Indeed, we observed altered expression of *Glutamate Signaling Pathway* proteins, and global synaptic protein co-expression was decreased in SCZ. However, network analysis also revealed *increased* expression and co-expression of glutamate-to-cytoskeleton signaling proteins as spine density *decreased* in SCZ. These findings were enabled by the unique perspective obtained from the concurrent quantification of 155 synaptic proteins and highlight the complexity of altered glutamate signaling in SCZ. Some of these changes are likely pathological, contributing to dendritic spine loss and auditory impairments in SCZ, while others may represent compensatory mechanisms.

Potential Caveats

First, we utilized a multiplexed approach to protein measurement, raising the possibility that multiple hypothesis testing could contribute to false positives in our findings. Thus, it should be noted that the pathway analysis finding that *Glutamate Signaling Pathway* proteins are amongst the most differentially expressed proteins survives formal correction for multiple hypothesis testing. Similarly, the permutation analysis of network connectivity is not subject to this limitation. Second, protein studies in human postmortem brain tissue are subject to potential confounding by the effect of technical factors such as PMI, clinical factors that vary within SCZ subjects such as suicide, schizoaffective disorder, and treatment history, and difficulty in matching control tissues on other potential variables such as tobacco and substance use. We used three approaches to attempt to mitigate these concerns. First, the SCZ cohort was matched as closely as possible to the control cohort on PMI and demographic factors (Supplemental Table S1). We have previously validated the stability of the proteins assayed by the LC-SRM/MS at a PMI of up to 24 hours(49), and our subjects did not significantly differ on this parameter. Second, we conducted post-hoc analyses to evaluate the effects of other potential confounds, and did not find an association of altered expression with tobacco use, suicide, substance abuse, schizoaffective disorder, or history of antipsychotic use in our subjects (Supplemental Table S6). Finally, to further control for the effects of antipsychotics on protein expression we utilized cortex tissue from monkeys

treated for 6 months with haloperidol or clozapine. The results of this experiment indicate that the differential expression of *Glutamate Signaling Pathway* proteins in SCZ is not likely attributable to therapeutic intervention. Indeed, antipsychotic drug treatment induced changes to GRIA4, ATP1A3 and GNAQ in reverse of those observed in SCZ (Figure 3), which may represent a possible therapeutic mechanism of action.

Glutamate Signaling Pathway Proteins

GRIA3 and GRIA4, the two most significantly dysregulated proteins in SCZ, are subunits of the hetero-tetramer ionotropic AMPA glutamate receptor(59, 60). AMPA receptor levels at the synapse are essential for long term potentiation (LTP) and spine maintenance(61). Thus the loss of these proteins could contribute to impairments in both. Indeed, evidence for altered AMPA receptor trafficking in SCZ has previously been observed in the frontal cortex(62). Furthermore, GRIA3 polymorphisms have been associated with increased risk for SCZ(63). In addition, GRIA3 mutations are a cause of intellectual disability(64), a syndrome that shares genetic risk with SCZ(65). Reduced GRIA3 (but not GRIA4) mRNA expression has previously been reported in thalamus in SCZ, but was not found to be reduced in prefrontal cortex(66, 67). Because most of the AMPA receptor population is localized somatodendritically(68), it is unlikely that thalamic projections to AI are the source of the reductions in GRIA3 protein we identified.

ATP1A3 is one of three alpha subunit variants of the ATP dependent NA^+/K^+ transporting channel expressed in the brain(69). ATP1A3 expression is neuron-specific, and is essential for returning neurons to the resting membrane potential after repeated firing(70). Decreased expression of ATP1A3 mRNA and protein in the prefrontal cortex has been observed in SCZ(71, 72). Rare mutations to ATP1A3 were recently identified as contributing to a polygenic burden for SCZ risk converging on the activity-regulated cytoskeleton-associated scaffold protein complex in the postsynaptic density(22). Mutations in ATP1A3 that reduce protein expression or activity are also strongly linked to rapid-onset dystonia-parkinsonism (RDP)(73, 74). The onset of RDP bears some similarities to that of first psychotic episodes in SCZ, including precipitation by an acute or sub-acute stressful event, sub-acute onset, and highest incidence of onset in the second decade of life(74). RDP patients with ATP1A3 mutations also display significant impairments in memory, attention, and executive function(75). 19% of RDP patients with an ATP1A3 mutation exhibited a psychotic syndrome characterized by auditory hallucinations(74), which occurred prior to or at onset of the motor symptoms. Indeed, we found that significant reductions in ATP1A3 levels were restricted to the subgroup of SCZ cases with a history of auditory hallucinations amongst their symptoms (Supplemental Figure S4).

It is not known if ATP1A3 reductions can induce glutamate signaling protein network abnormalities such as those we observed, or dendritic spine loss. However, ATP1A3 is present at dendritic spines(76, 77) where it interacts with PSD95(76, 77) and regulates transient Na^+ currents(78, 79), which effect NMDA receptor phosphorylation and activity through a src dependent mechanism(79). ATP1A3 +/− mice, in which ATP1A3 protein reduction is comparable to what we observed in SCZ, display memory impairments, increased sensitivity to amphetamines, and a 40% reduction in GRIN1 in the hippocampus,

demonstrating that ATP1A3 reduction impacts psychosis relevant phenotypes and glutamate signaling protein networks(80). Additionally, there is evidence suggesting that application of ouabain at concentrations selective for ATP1A3 (relative to ATP1A1) induces degradation of AMPA receptors via internalization and targeting to the ubiquitin-proteosome system(81). Thus, it is possible that reduction of ATP1A3 is upstream of the GRIA protein reductions we observed, a hypothesis that could be tested in the ATP1A3 +/− model. Genetic models of ATP1A3 and GRIA3 reduction would also provide a robust source for unbiased proteomic discovery of additional glutamate signaling network alterations that could then be forward translated into hypothesis testing in human tissue.

In addition to *Glutamate Signaling Pathway* proteins, we observed alterations to additional molecules previously implicated in SCZ. We have previously observed decreased GAD65(82) in the Al of SCZ patients. These decreases, measured at layer 3 inhibitory boutons, were much greater than those observed in whole tissue homogenates(82), suggesting that alterations to other proteins observed in the present study may be greater within specific neuronal microdomain. We also observed differences in expression of the ubiquitin/proteasome pathway proteins UCHL1 and PSMA1, which have previously been implicated in SCZ(83). These reports further validate the alterations we observed in these molecules and pathways, and support current interest in them.

Co-expression network topology is altered in SCZ

When protein levels of two genes are correlated across a cohort, they are “co-expressed”. Proteins that are tightly and mutually co-expressed within a network, referred to as a module, are often functionally related. Co-expression can result from one or more coordinated biological functions, such as a shared promoter, chromosomal proximity, shared degradation, or expression in specific cell populations within the tissue sample(84). Differences in network features between control and disease cohorts can represent alterations to one or more of these functions. Thus, they represent a unique way to evaluate a complex data set in a non-reductionist perspective and have provided valuable insight in a number of neuropsychiatric diseases(85–87).

Here we used expression data from 155 proteins to construct and compare protein co-expression networks for SCZ and control cohorts. We observed two significant differences between these networks. First, global protein co-expression is significantly decreased in the SCZ cohort (Figure 1, Supplemental Figure S3). This loss of protein co-expression in SCZ could be due to the loss of coordinated biological activity, such as alterations in the relative amounts of cell types or neuronal connections in SCZ compared to controls, or a loosening of gene expression regulation. Alternatively, decreased protein co-expression in the SCZ population, compared to controls, could be due to the heterogeneity of the disease itself. That is, the SCZ cohort studied here could include a number of disease subtypes each with a distinct co-expression network topology.

Second, we observed an emergent module in the SCZ group not present in the controls (Figure 1). Functional Gene Annotation analysis strongly suggests that the extended construct of this emergent module is involved in the transduction of glutamate signals to the cytoskeleton within spines. Indeed, this extended module includes DLG4 (PSD95) and

SYNGAP, two of the most abundant proteins in the postsynaptic density(88). Additionally, all of the core proteins in the emergent module are also highly enriched in postsynaptic structures within spines(49), serving to link scaffolding proteins, such as DLG4, to the cytoskeleton. The average expression values of the extended emergent network were significantly inversely correlated with spine density in SCZ, but not controls (Figure 2), indicating that this module has a disease specific relationship to the pathology of spine loss. This module could be the result of an attempted compensatory mechanism, activated in face of spine loss in SCZ. Alternatively, pathological impairments in coordinated protein degradation could also explain this observation as proteasome activity regulates postsynaptic density protein abundances(89) and is essential for both spine formation and retraction(90, 91).

Conclusion

This is the first study utilizing a targeted proteomics approach to identify aberrant glutamate signaling protein network features and link them to spine loss in SCZ. Future studies to investigate if these alterations are unique to the AI or present in other brain areas implicated in disease are needed. Furthermore, additional studies will be required to enhance the interpretation of these findings by examining whether they are global or cell type specific changes. For example, GRIA3 is expressed post-synaptically in both glutamatergic and gabaergic neurons,(68) such that the effects of reduced expression will differ substantially if only one cell population is affected. Multiple label quantitative fluorescence microscopy provides one approach to relative quantification of selected protein levels with cell type specificity(82, 92–94). In addition, circuitry and function in the cerebral cortex, including AI, has a laminar organization(95), and the cytoarchitecture of layer 3 may be more affected than others in SCZ(34). Collection and subsequent LC-SRM/SRM analysis of individual grey matter layers by laser capture is feasible(96, 97), and would enhance discovery of protein alterations linked to layer-specific abnormalities. Thus, combining layer-based proteomic discovery with follow-up multiple label quantitative fluorescence microscopy evaluation would provide a robust approach to evaluating protein alterations in post-mortem tissue, allowing for the construction of more detailed reverse genetic models.

Supplementary Material

Refer to Web version on PubMed Central for supplementary material.

Acknowledgments

This work was funded by National Institutes of Health grants MH 071533 and T32 MH 16804. The Biomedical Mass Spectrometry Center and UPCI Cancer Biomarker Facility are supported in part by award P30CA047904.

References

1. Voisin J, Bidet-Caulet A, Bertrand O, Fonlupt P. Listening in silence activates auditory areas: a functional magnetic resonance imaging study. J Neurosci. 2006; 26:273–278. [PubMed: 16399697]
2. Copolov DL, Seal ML, Maruff P, Ulusoy R, Wong MT, Tochon-Danguy HJ, et al. Cortical activation associated with the experience of auditory hallucinations and perception of human speech

in schizophrenia: a PET correlation study. Psychiatry Research. 2003; 122:139–152. [PubMed: 12694889]

3. Gaser C, Nenadic I, Volz HP, Buchel C, Sauer H. Neuroanatomy of “hearing voices”: a frontotemporal brain structural abnormality associated with auditory hallucinations in schizophrenia. CerebCortex. 2004; 14:91–96.
4. Lawrie SM, Buechel C, Whalley HC, Frith CD, Friston KJ, Johnstone EC. Reduced frontotemporal functional connectivity in schizophrenia associated with auditory hallucinations. Biological Psychiatry. 2002; 51:1008–1011. [PubMed: 12062886]
5. Shergill SS, Brammer MJ, Williams SCR, Murray RM, McGuire PK. Mapping auditory hallucinations in schizophrenia using functional magnetic resonance imaging. Archives of General Psychiatry. 2000; 57:1033–1038. [PubMed: 11074868]
6. Javitt DC, Doneshka P, Grochowski S, Ritter W. Impaired mismatch negativity generation reflects widespread dysfunction of working memory in schizophrenia. Archives of General Psychiatry. 1995; 52:550–558. [PubMed: 7598631]
7. Javitt DC, Strous RD, Grochowski S, Ritter W, Cowan N. Impaired precision, but normal retention, of auditory sensory (“echoic”) memory information in schizophrenia. Journal of Abnormal Psychology. 1997; 106:315–324. [PubMed: 9131851]
8. Javitt DC, Shelley AM, Ritter W. Associated deficits in mismatch negativity generation and tone matching in schizophrenia. ClinNeurophysiol. 2000; 111:1733–1737.
9. Rabinowicz EF, Silipo G, Goldman R, Javitt DC. Auditory sensory dysfunction in schizophrenia. Imprecision or distractibility? Archives of General Psychiatry. 2000; 57:1149–1155. [PubMed: 11115328]
10. Leitman DI, Foxe JJ, Butler PD, Saperstein A, Revheim N, Javitt DC. Sensory contributions to impaired prosodic processing in schizophrenia. Biological Psychiatry. 2005; 58:56–61. [PubMed: 15992523]
11. Leitman DI, Laukka P, Juslin PN, Saccente E, Butler P, Javitt DC. Getting the cue: sensory contributions to auditory emotion recognition impairments in schizophrenia 18. SchizophrBull. 2010; 36:545–556.
12. Gold R, Butler P, Revheim N, Leitman DI, Hansen JA, Gur RC, et al. Auditory emotion recognition impairments in schizophrenia: relationship to acoustic features and cognition. Am J Psychiatry. 2012; 169:424–432. [PubMed: 22362394]
13. Kantrowitz JT, Leitman DI, Lehrfeld JM, Laukka P, Juslin PN, Butler PD, et al. Reduction in tonal discriminations predicts receptive emotion processing deficits in schizophrenia and schizoaffective disorder. SchizophrBull. 2013; 39:86–93.
14. Shelley AM, Silipo G, Javitt DC. Diminished responsiveness of ERPs in schizophrenic subjects to changes in auditory stimulation parameters: implications for theories of cortical dysfunction. Schizophrenia Research. 1999; 37:65–79. [PubMed: 10227109]
15. Ahveninen J, Jääskeläinen IP, Osipova D, Huttunen MO, Ilmoniemi RJ, Kaprio J, et al. Inherited auditory-cortical dysfunction in twin pairs discordant for schizophrenia. Biological Psychiatry. 2006; 60:612–620. [PubMed: 16876141]
16. Javitt DC, Steinschneider M, Schroeder CE, Vaughan JHG, Arezzo JC. Detection of stimulus deviance within primate primary auditory cortex: intracortical mechanisms of mismatch negativity (MMN) generation. Brain Research. 1994; 667:192–200. [PubMed: 7697356]
17. Javitt DC, Steinschneider M, Schroeder CE, Arezzo JC. Role of cortical N-methyl-D-aspartate receptors in auditory sensory memory and mismatch negativity generation: implications for schizophrenia. Proceeding of the National Academy of Sciences of the United States of America. 1996; 93:11962–11967.
18. Umbricht D, Schmid L, Koller R, Vollenweider FX, Hell D, Javitt DC. Ketamine-induced deficits in auditory and visual context-dependent processing in healthy volunteers: implications for models of cognitive deficits in schizophrenia. Arch GenPsychiatry. 2000; 57:1139–1147.
19. Gunduz-Bruce H, Reinhart RM, Roach BJ, Gueorguieva R, Oliver S, D’Souza DC, et al. Glutamatergic modulation of auditory information processing in the human brain. Biol Psychiatry. 2012; 71:969–977. [PubMed: 22036036]

20. Ehrlichman RS, Maxwell CR, Majumdar S, Siegel SJ. Deviance-elicited changes in event-related potentials are attenuated by ketamine in mice. J Cogn Neurosci. 2008; 20:1403–1414. [PubMed: 18303985]
21. Malhotra AK, Pinals DA, Adler CM, Elman I, Clifton A, Pickar D, et al. Ketamine-induced exacerbation of psychotic symptoms and cognitive impairment in neuroleptic-free schizophrenics. Neuropsychopharmacology. 1997; 17:141–150. [PubMed: 9272481]
22. Purcell SM, Moran JL, Fromer M, Ruderfer D, Solovieff N, Roussos P, et al. A polygenic burden of rare disruptive mutations in schizophrenia. Nature. 2014; 506:185–190. [PubMed: 24463508]
23. Fromer M, Pocklington AJ, Kavanagh DH, Williams HJ, Dwyer S, Gormley P, et al. De novo mutations in schizophrenia implicate synaptic networks. Nature. 2014; 506:179–184. [PubMed: 24463507]
24. Kirov G, Pocklington AJ, Holmans P, Ivanov D, Ikeda M, Ruderfer D, et al. De novo CNV analysis implicates specific abnormalities of postsynaptic signalling complexes in the pathogenesis of schizophrenia. Molecular Psychiatry. 2011:1–12. [PubMed: 21483438]
25. Fernández, EFa; Collins, MO.; Uren, RT.; Kopanitsa, MV.; Komiyama, NH.; Croning, MDR., et al. Targeted tandem affinity purification of PSD-95 recovers core postsynaptic complexes and schizophrenia susceptibility proteins. Molecular Systems Biology. 2009; 5:1–17.
26. Thaker GK. Neurophysiological endophenotypes across bipolar and schizophrenia psychosis. Schizophr Bull. 2008; 34:760–773. [PubMed: 18502737]
27. Lewis DA, Sweet RA. Schizophrenia from a neural circuitry perspective: advancing toward rational pharmacological therapies. Journal of Clinical Investigation. 2009; 119:706–716. [PubMed: 19339762]
28. Glantz LA, Lewis DA. Decreased dendritic spine density on prefrontal cortical pyramidal neurons in schizophrenia. Archives of General Psychiatry. 2000; 57:65–73. [PubMed: 10632234]
29. Kalus P, Müller TJ, Zuschratter W, Senitz D. The dendritic architecture of prefrontal pyramidal neurons in schizophrenic patients. Neuroreport. 2000; 11:3621–3625. [PubMed: 11095531]
30. Black JE, Kodish IM, Grossman AW, Klintsova AY, Orlovskaya D, Vostrikov V, et al. Pathology of layer V pyramidal neurons in the prefrontal cortex of patients with schizophrenia 1. American Journal of Psychiatry. 2004; 161:742–744. [PubMed: 15056523]
31. Broadbelt K, Byne W, Jones LB. Evidence for a decrease in basilar dendrites of pyramidal cells in schizophrenic medial prefrontal cortex 3. SchizophrRes. 2002; 58:75–81.
32. Pierri JN, Volk CL, Auh S, Sampson A, Lewis DA. Decreased somal size of deep layer 3 pyramidal neurons in the prefrontal cortex of subjects with schizophrenia. Archives of General Psychiatry. 2001; 58:466–473. [PubMed: 11343526]
33. Sweet RA, Pierri JN, Auh S, Sampson AR, Lewis DA. Reduced pyramidal cell somal volume in auditory association cortex of subjects with schizophrenia. Neuropsychopharmacology. 2003; 28:599–609. [PubMed: 12629543]
34. Sweet RA, Bergen SE, Sun Z, Sampson AR, Pierri JN, Lewis DA. Pyramidal cell size reduction in schizophrenia: evidence for involvement of auditory feedforward circuits. Biological Psychiatry. 2004; 55:1128–1137. [PubMed: 15184031]
35. Sweet RA, Henteleff RA, Zhang W, Sampson AR, Lewis DA. Reduced dendritic spine density in auditory cortex of subjects with schizophrenia. Neuropsychopharmacology : official publication of the American College of Neuropsychopharmacology. 2009; 34:374–389. [PubMed: 18463626]
36. Garey LJ, Ong WY, Patel TS, Kanani M, Davis A, Mortimer AM, et al. Reduced dendritic spine density on cerebral cortical pyramidal neurons in schizophrenia. Journal of Neurology, Neurosurgery and Psychiatry. 1998; 65:446–453.
37. Chen X, Leischner U, Rochefort NL, Nelken I, Konnerth A. Functional mapping of single spines in cortical neurons in vivo. Nature. 2011; 475:501–505. [PubMed: 21706031]
38. Midtgaard J. The integrative properties of spiny distal dendrites. Neuroscience. 1992; 50:501–502. [PubMed: 1436501]
39. Sheppard JM, Woolf TB, Carnevale NT. Comparisons between Active Properties of Distal Dendritic Branches and Spines: Implications for Neuronal Computations. Journal of Cognitive Neuroscience. 1989; 1:273–286. [PubMed: 23968510]

40. Tsay D, Yuste R. On the electrical function of dendritic spines. Trends Neurosci. 2004; 27:77–83. [PubMed: 15102486]
41. Meng Y, Zhang Y, Jia Z. Synaptic transmission and plasticity in the absence of AMPA glutamate receptor GluR2 and GluR3. Neuron. 2003; 39:163–176. [PubMed: 12848940]
42. Ultanir SK, Kim JE, Hall BJ, Deerinck T, Ellisman M, Ghosh A. Regulation of spine morphology and spine density by NMDA receptor signaling in vivo. Proceedings of the National Academy of Sciences of the United States of America. 2007; 104:19553–19558. [PubMed: 18048342]
43. McKinney RA, Capogna M, Durr R, Gahwiler BH, Thompson SM. Miniature synaptic events maintain dendritic spines via AMPA receptor activation. NatNeurosci. 1999; 2:44–49.
44. Cheng HW, Rafols JA, Goshgarian HG, Anavi Y, Tong J, McNeill TH. Differential spine loss and regrowth of striatal neurons following multiple forms of deafferentation: a Golgi study. ExpNeurol. 1997; 147:287–298.
45. Matthews DA, Cotman C, Lynch G. An electron microscopic study of lesion-induced synaptogenesis in the dentate gyrus of the adult rat. II. Reappearance of morphologically normal synaptic contacts. Brain Res. 1976; 115:23–41. [PubMed: 974742]
46. Li L, Chin LS, Shupliakov O, Brodin L, Sihra TS, Hvalby O, et al. Impairment of synaptic vesicle clustering and of synaptic transmission, and increased seizure propensity, in synapsin I-deficient mice. Proc Natl Acad Sci USA. 1995; 92:9235–9239. [PubMed: 7568108]
47. Kwon SE, Chapman ER. Synaptophysin regulates the kinetics of synaptic vesicle endocytosis in central neurons. Neuron. 2011; 70:847–854. [PubMed: 21658579]
48. Balu DT, Basu AC, Corradi JP, Cacace AM, Coyle JT. The NMDA receptor co-agonists, d-serine and glycine, regulate neuronal dendritic architecture in the somatosensory cortex. Neurobiology of disease. 2011:1–12.
49. Macdonald ML, Ciccimaro E, Prakash A, Banerjee A, Seeholzer SH, Blair IA, et al. Biochemical fractionation and stable isotope dilution liquid chromatography-mass spectrometry for targeted and microdomain-specific protein quantification in human postmortem brain tissue. Mol Cell Proteomics. 2012; 11:1670–1681. [PubMed: 22942359]
50. Huang, dW; Sherman, BT.; Lempicki, RA. Systematic and integrative analysis of large gene lists using DAVID bioinformatics resources. Nat Protoc. 2009; 4:44–57. [PubMed: 19131956]
51. Shelton, MA.; Newman, JT.; Fish, KN.; Penzes, P.; Lewis, DA.; Sweet, RA. Society for Neuroscience. San Diego, CA: 2013. Schizophrenia-associated alterations of microtubule associated protein 2 in human auditory cortex.
52. Glantz LA, Lewis DA. Decreased dendritic spine density on prefrontal cortical pyramidal neurons in schizophrenia. Archives of General Psychiatry. 2000; 57:65–73. [PubMed: 10632234]
53. O'Connor JA, Hasenkamp W, Horman BM, Muly EC, Hemby SE. Region specific regulation of NR1 in rhesus monkeys following chronic antipsychotic drug administration. Biological Psychiatry. 2006; 60:659–662. [PubMed: 16806093]
54. O'Connor JA, Muly EC, Arnold SE, Hemby SE. AMPA receptor subunit and splice variant expression in the DLPFC of schizophrenic subjects and rhesus monkeys chronically administered antipsychotic drugs. Schizophrenia Research. 2007; 90:28–40. [PubMed: 17141476]
55. Deo AJ, Cahill ME, Li S, Goldszer I, Henteleff R, Vanleeuwen JE, et al. Increased expression of Kalirin-9 in the auditory cortex of schizophrenia subjects: Its role in dendritic pathology. Neurobiology of disease. 2011
56. Deo AJ, Goldszer IM, Li S, DiBitetto JV, Henteleff RA, Sampson AR, et al. PAK1 Protein Expression in the Auditory Cortex of Schizophrenia Subjects. PLoS One. 2013; 8:e59458. [PubMed: 23613712]
57. Huang da W, Sherman BT, Lempicki RA. Systematic and integrative analysis of large gene lists using DAVID bioinformatics resources. Nature protocols. 2009; 4:44–57.
58. Langfelder P, Horvath S. WGCNA: an R package for weighted correlation network analysis. BMC Bioinformatics. 2008; 9:559. [PubMed: 19114008]
59. Traynelis SF, Wollmuth LP, McBain CJ, Menniti FS, Vance KM, Ogden KK, et al. Glutamate receptor ion channels: structure, regulation, and function. Pharmacol Rev. 2010; 62:405–496. [PubMed: 20716669]

60. Dingledine R, Borges K, Bowie D, Traynelis SF. The glutamate receptor ion channels. Pharmacol Rev. 1999; 51:7–61. [PubMed: 10049997]
61. Malinow R, Malenka RC. AMPA receptor trafficking and synaptic plasticity. Annu Rev Neurosci. 2002; 25:103–126. [PubMed: 12052905]
62. Hammond JC, McCullumsmith RE, Haroutunian V, Meador-Woodruff JH. Endosomal trafficking of AMPA receptors in frontal cortex of elderly patients with schizophrenia. Schizophrenia Research. 2011:1–6.
63. Magri C, Gardella R, Valsecchi P, Barlati SD, Guizzetti L, Imperadori L, et al. Study on GRIA2, GRIA3 and GRIA4 genes highlights a positive association between schizophrenia and GRIA3 in female patients. Am J Med Genet B Neuropsychiatr Genet. 2008; 147B:745–753. [PubMed: 18163426]
64. Wu Y, Arai AC, Rumbaugh G, Srivastava AK, Turner G, Hayashi T, et al. Mutations in ionotropic AMPA receptor 3 alter channel properties and are associated with moderate cognitive impairment in humans. Proc Natl Acad Sci U S A. 2007; 104:18163–18168. [PubMed: 17989220]
65. Cross-Disorder Group of the Psychiatric Genomics C Genetic Risk Outcome of Psychosis C . Identification of risk loci with shared effects on five major psychiatric disorders: a genome-wide analysis. Lancet. 2013; 381:1371–1379. [PubMed: 23453885]
66. Beneyto M, Meador-Woodruff JH. Lamina-specific abnormalities of AMPA receptor trafficking and signaling molecule transcripts in the prefrontal cortex in schizophrenia. Synapse. 2006; 60:585–598. [PubMed: 16983646]
67. Ibrahim HM, Hogg AJ Jr, Healy DJ, Haroutunian V, Davis KL, Meador-Woodruff JH. Ionotropic glutamate receptor binding and subunit mRNA expression in thalamic nuclei in schizophrenia. Am J Psychiatry. 2000; 157:1811–1823. [PubMed: 11058479]
68. Moga DE, Janssen WG, Vissavajjhala P, Czelusniak SM, Moran TM, Hof PR, et al. Glutamate receptor subunit 3 (GluR3) immunoreactivity delineates a subpopulation of parvalbumin-containing interneurons in the rat hippocampus. J Comp Neurol. 2003; 462:15–28. [PubMed: 12761821]
69. Henriksen C, Kjaer-Sorensen K, Einholm AP, Madsen LB, Momeni J, Bendixen C, et al. Molecular Cloning and Characterization of Porcine Na(+)/K(+)-ATPase Isoforms alpha1, alpha2, alpha3 and the ATP1A3 Promoter. PLoS One. 2013; 8:e79127. [PubMed: 24236096]
70. Dobretsov M, Stimers JR. Neuronal function and alpha3 isoform of the Na/K-ATPase. Frontiers in bioscience : a journal and virtual library. 2005; 10:2373–2396. [PubMed: 15970502]
71. English JA, Pennington K, Dunn MJ, Cotter DR. The neuroproteomics of schizophrenia. Biological Psychiatry. 2011; 69:163–172. [PubMed: 20887976]
72. Tochigi M, Iwamoto K, Bundo M, Sasaki T, Kato N, Kato T. Gene expression profiling of major depression and suicide in the prefrontal cortex of postmortem brains. Neurosci Res. 2008; 60:184–191. [PubMed: 18068248]
73. de Carvalho Aguiar P, Sweadner KJ, Penniston JT, Zaremba J, Liu L, Caton M, et al. Mutations in the Na+/K+-ATPase alpha3 gene ATP1A3 are associated with rapid-onset dystonia parkinsonism. Neuron. 2004; 43:169–175. [PubMed: 15260953]
74. Brashear A, Cook JF, Hill DF, Amponsah A, Snively BM, Light L, et al. Psychiatric disorders in rapid-onset dystonia-parkinsonism. Neurology. 2012; 79:1168–1173. [PubMed: 22933743]
75. Cook JF, Hill DF, Snively BM, Boggs N, Suerken CK, Haq I, et al. Cognitive impairment in rapid-onset dystonia-parkinsonism. Movement disorders : official journal of the Movement Disorder Society. 2014
76. Azarias G, Kruusmagi M, Connor S, Akkuratov EE, Liu XL, Lyons D, et al. A specific and essential role for Na,K-ATPase alpha3 in neurons co-expressing alpha1 and alpha3. J Biol Chem. 2013; 288:2734–2743. [PubMed: 23195960]
77. Blom H, Ronnlund D, Scott L, Spicarova Z, Widengren J, Bondar A, et al. Spatial distribution of Na+-K+-ATPase in dendritic spines dissected by nanoscale superresolution STED microscopy. BMC neuroscience. 2011; 12:16. [PubMed: 21272290]
78. Rose CR, Konnerth A. NMDA receptor-mediated Na+ signals in spines and dendrites. J Neurosci. 2001; 21:4207–4214. [PubMed: 11404406]

79. Yu XM, Salter MW. Gain control of NMDA-receptor currents by intracellular sodium. Nature. 1998; 396:469–474. [PubMed: 9853755]
80. Moseley AE, Williams MT, Schaefer TL, Bohanan CS, Neumann JC, Behbehani MM, et al. Deficiency in Na,K-ATPase alpha isoform genes alters spatial learning, motor activity, and anxiety in mice. J Neurosci. 2007; 27:616–626. [PubMed: 17234593]
81. Zhang D, Hou Q, Wang M, Lin A, Jarzylo L, Navis A, et al. Na,K-ATPase activity regulates AMPA receptor turnover through proteasome-mediated proteolysis. J Neurosci. 2009; 29:4498–4511. [PubMed: 19357275]
82. Moyer CE, Delevich KM, Fish KN, Asafu-Adjei JK, Sampson AR, Dorph-Petersen KA, et al. Reduced Glutamate Decarboxylase 65 Protein Within Primary Auditory Cortex Inhibitory Boutons in Schizophrenia. Biol Psychiatry. 2012
83. Rubio MD, Wood K, Haroutunian V, Meador-Woodruff JH. Dysfunction of the ubiquitin proteasome and ubiquitin-like systems in schizophrenia. Neuropsychopharmacology. 2013; 38:1910–1920. [PubMed: 23571678]
84. Gaiteri C, Ding Y, French B, Tseng GC, Sibille E. Beyond modules and hubs: the potential of gene coexpression networks for investigating molecular mechanisms of complex brain disorders. Genes Brain Behav. 2014; 13:13–24. [PubMed: 24320616]
85. Sibille E, Wang Y, Joeyen-Waldorf J, Gaiteri C, Surget A, Oh S, et al. A molecular signature of depression in the amygdala. AmJ Psychiatry. 2009; 166:1011–1024. [PubMed: 19605536]
86. Gaiteri C, Sibille E. Differentially expressed genes in major depression reside on the periphery of resilient gene coexpression networks. Front Neurosci. 2011; 5:95. [PubMed: 21922000]
87. Chen C, Cheng L, Grennan K, Pibiri F, Zhang C, Badner JA, et al. Two gene co-expression modules differentiate psychotics and controls. Mol Psychiatry. 2013; 18:1308–1314. [PubMed: 23147385]
88. Cheng D, Hoogenraad CC, Rush J, Ramm E, Schlager MA, Duong DM, et al. Relative and absolute quantification of postsynaptic density proteome isolated from rat forebrain and cerebellum. Molecular & cellular proteomics : MCP. 2006; 5:1158–1170. [PubMed: 16507876]
89. Ehlers MD. Activity level controls postsynaptic composition and signaling via the ubiquitin-proteasome system. Nature Neuroscience. 2003; 6:231–242.
90. Hamilton AM, Oh WC, Vega-Ramirez H, Stein IS, Hell JW, Patrick GN, et al. Activity-Dependent Growth of New Dendritic Spines Is Regulated by the Proteasome. Neuron. 2012; 74:1023–1030. [PubMed: 22726833]
91. Erturk A, Wang Y, Sheng M. Local pruning of dendrites and spines by caspase-3-dependent and proteasome-limited mechanisms. J Neurosci. 2014; 34:1672–1688. [PubMed: 24478350]
92. Moyer CE, Delevich KM, Fish KN, Asafu-Adjei JK, Sampson AR, Dorph-Petersen KA, et al. Intracortical excitatory and thalamocortical boutons are intact in primary auditory cortex in schizophrenia. SchizophrRes. 2013
93. Fish KN, Sweet RA, Deo AJ, Lewis DA. An automated segmentation methodology for quantifying immunoreactive puncta number and fluorescence intensity in tissue sections. Brain Res. 2008; 1240:62–72. [PubMed: 18793619]
94. Fish KN, Sweet RA, Lewis DA. Differential distribution of proteins regulating GABA synthesis and reuptake in axon boutons of subpopulations of cortical interneurons 1. Cereb Cortex. 2011; 21:2450–2460. [PubMed: 21422269]
95. Linden JF, Schreiner CE. Columnar transformations in auditory cortex? A comparison to visual and somatosensory cortices. Cereb Cortex. 2003; 13:83–89. [PubMed: 12466219]
96. Arion D, Horvath S, Lewis DA, Mirnics K. Infragranular gene expression disturbances in the prefrontal cortex in schizophrenia: signature of altered neural development? Neurobiol Dis. 2010; 37:738–746. [PubMed: 20034564]
97. Pennington K, Dicker P, Dunn MJ, Cotter DR. Proteomic analysis reveals protein changes within layer 2 of the insular cortex in schizophrenia. Proteomics. 2008; 8:5097–5107. [PubMed: 19003868]

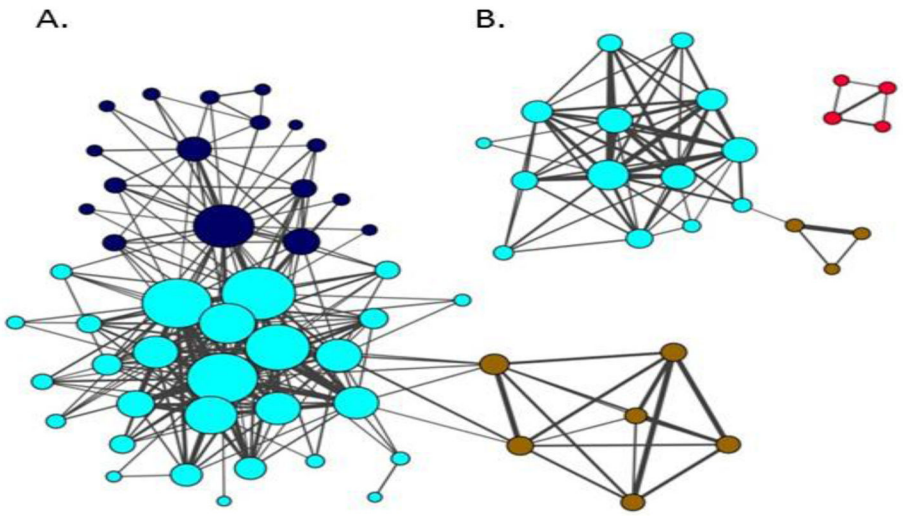

Figure 1. Protein co-expression is altered in the AI of SCZ

Protein co-expression networks were constructed for control (A) and SCZ (B) cohorts. Each node (circle) represents a protein. Color denotes membership in module as defined by connectivity. Node sizes are proportional to proteins' degree of connectivity. Line weights represent between-protein correlations. SCZ and control networks are rendered on same scale. Only proteins with a weighted Node connectivity > .15 were included the networks. The three modules composing the control network are characterized by function/ compartment. Blue: vesicular, Turquiose: Catabolism/Cytoplasm, Brown: Apoptosis. Two of these modules are conserved, albeit smaller and less connected, in the SCZ network. The Red module, composed of postsynaptic density proteins, is unique to SCZ. The SCZ network had lower global connectivity (p=0.015). Network/Module membership is reported in Supplemental Table 3.

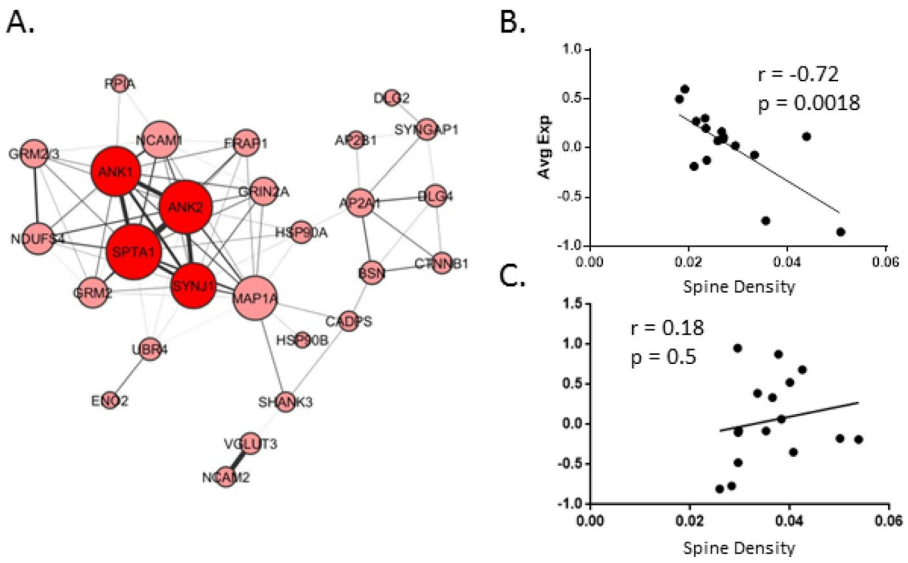

Figure 2. Schizophrenia Specific Module

A. shows a visualization of the SCZ specific Red module from Figure 2 with the Node Degree Requirement for visualization loosened to 0.1. **B.** shows the average expression of the proteins comprising this module plotted against spine density in the SCZ cohort, and **C.** the same for the control cohort.

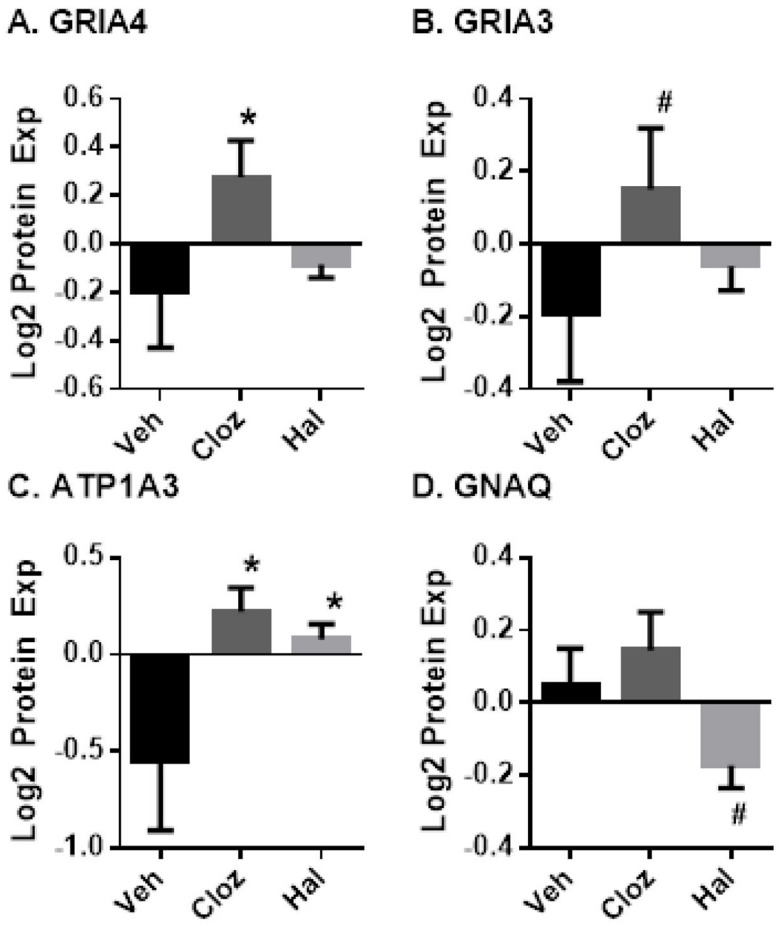

Figure 3. Chronic Antipsychotic Drug Treatment Effects on *Glutamate Signaling Pathway* Proteins in Rhesus Monkeys

Rhesus monkeys were treated for six months with vehicle, haloperidol or clozapine. Protein expression in grey matter homogenates was measured by LC-SRM/MS. Error bars: standard error of the mean; #: $p < 0.01$ vs vehicle, *: $p < 0.05$ vs vehicle.

Table 1

Summary of Subject Characteristics

There were no diagnostic group differences in age, sex, postmortem interval, storage time, or in the distribution of handedness between the diagnostic groups. There was a small but significant difference in pH.

	Control	Schizophrenia	p
N	23	22	
Mean Age (SD)	45.8 (11.3)	47.2 (13.7)	0.71
Range	19–67	25–71	
Sex (F/M)	5/18	5/17	
Handedness (R/L/M/U)	21/2	14/3/1/4	
PMI (SD)	17.9 (6.6)	18.9 (8.1)	0.64
Storage Time, mos (SD)	130 (43)	126 (37)	0.69
pH(SD)	6.7 (0.3)	6.5 (0.3)	0.045
Suicide, N (%)		7 (32%)	
Schizoaffective, N (%)		7 (32%)	
Alcohol/Substance abuse ATOD, N (%)		15 (68%)	
Antipsychotic AT OD, N (%)		19 (86%)	

A, ambidextrous; F, female; L, left-handed; M, male; PMI, postmortem interval; R, right-handed; U, unknown.

Table 2

Differentially expressed proteins in Al gray matter homogenates, as measured by LC-SRM/MS

Proteins are denoted by common gene symbols. All proteins with an ANCOVA p-value < 0.1 are shown. Bolded proteins are members of the *Glutamate Signaling Pathway*.

Protein	SCZ/CTL	P	CV
GRIA4	0.69	0.0004	0.123
GRIA3	0.72	0.0139	0.032
ATP1A3	0.93	0.0189	0.022
PHB2	0.95	0.0323	0.012
UCHL1	1.1	0.0412	0.008
VIM	0.9	0.0425	0.02
HSP90B	0.89	0.0576	0.043
PSMA1	1.1	0.0594	0.007
GAD65	0.9	0.0598	0.063
GNAQ	1.2	0.0611	0.042
NDUFV1	0.93	0.0662	0.022
SYN1	0.88	0.0696	0.019
PRKCA	0.86	0.0792	0.006
PC	0.77	0.0831	0.063
DNM1	1.13	0.0899	0.024
CTNNB1	1.12	0.092	0.009
ATP5A1	0.93	0.0923	0.019

CTL- Control. CV- coefficient of variation.